JOURNAL OF VIROLOGY, July 2005, p. 8602–8613 Vol. 79, No. 13
0022-538X/05/$08.00+0 doi:10.1128/JVI.79.13.8602–8613.2005


# Attenuation of Recombinant Yellow Fever 17D Viruses Expressing Foreign Protein Epitopes at the Surface

Myrna C. Bonaldo,[1] Richard C. Garratt,[2] Renato S. Marchevsky,[3] Evandro S. F. Coutinho,[4] Alfredo V. Jabor,[1] Luís F. C. Almeida,[3] Anna M. Y. Yamamura,[3] Adriana S. Duarte,[1] Prisciliana J. Oliveira,[1] Jackeline O. P. Lizeu,[1] Luiz A. B. Camacho,[4] Marcos S. Freire,[3] and Ricardo Galler[1]*

*Fundação Oswaldo Cruz, Instituto Oswaldo Cruz, Departamento de Bioquimica e Biologia Molecular,[1] Fundação Oswaldo Cruz, Instituto de Tecnologia em Imunobiológicos, Departamento de Controle de Qualidade,[3] and Escola Nacional de Saúde Pública,[4] Rio de Janeiro, and Universidade de São Paulo, Instituto de Física de São Carlos, São Carlos,[2] Brazil*

Received 26 November 2004/Accepted 13 March 2005

**The yellow fever (YF) 17D vaccine is a live attenuated virus. Three-dimensional (3D) homology modeling of the E protein structure from YF 17D virus and its comparison with that from tick-borne encephalitis virus revealed that it is possible to accommodate inserts of different sizes and amino acid compositions in the flavivirus E protein *fg* loop. This is consistent with the 3D structures of both the dimeric and trimeric forms in which the *fg* loop lies exposed to solvents. We demonstrate here that YF 17D viruses bearing foreign humoral (17D/8) and T-cell (17D/13) epitopes, which vary in sequence and length, displayed growth restriction. It is hypothesized that interference with the dimer-trimer transition and with the formation of a ring of such trimers in order to allow fusion compromises the capability of the E protein to induce fusion of viral and endosomal membranes, and a slower rate of fusion may delay the extent of virus production. This would account for the lower levels of replication in cultured cells and of viremia in monkeys, as well as for the more attenuated phenotype of the recombinant viruses in monkeys. Testing of both recombinant viruses (17D/8 and 17D/13) for monkey neurovirulence also suggests that insertion at the 17D E protein *fg* loop does not compromise the attenuated phenotype of YF 17D virus, further confirming the potential use of this site for the development of new live attenuated 17D virus-based vaccines.**

The yellow fever (YF) 17D virus is attenuated and used for human vaccination. Some of the outstanding properties of this vaccine include limited viral replication in the host but with significant expansion and dissemination of the viral mass, yielding a robust and long-lived neutralizing antibody response. The vaccine is cheap and applied as a single dose, and there are well-established production methodology and quality control procedures, which include the monkey neurovirulence test (MNVT). Altogether, the 17D virus has become very attractive as an expression vector for the development of new live attenuated vaccines.

The development of infectious-clone technology has allowed the genetic manipulation of the YF 17D virus genome toward the expression of foreign genes. Different technical approaches to constructing recombinant viruses based on the YF 17D virus are possible and will differ according to the antigen to be expressed. One major approach has been the creation of chimeric viruses through the exchange of structural prM/M/E genes (reviewed in reference 10). An alternative approach used in the development of YF 17D virus as a vector for heterologous antigens is the expression of particular epitopes in the E protein. In the mature virus, the E protein forms a symmetrical network of 90 dimers. These dimers are anchored into the viral envelope and lie flat on its surface. Each monomer is composed of three domains. The central and dimerization domains (I and II, respectively) are formed of several noncontiguous stretches of the polypeptide chain, while the C-terminal domain III is a continuous immunoglobulin-like module that leads into the stem section and subsequently the transmembrane helices (22). Domain III is implicated in mediating cell receptor recognition and cell penetration (17, 21, 22).

We have previously described the viability of heterologous insertions in the *fg* loop of the YF 17D virus E protein (1). This loop is located in domain II, distant from the receptor binding domain III. Hence, insertions in the former should not alter attenuation for humans and monkeys, which is a major characteristic of YF 17D virus. We have formerly used this *fg* loop site for the insertion of a model humoral epitope from the circumsporozoite (CS) surface protein from the protozoan parasite *Plasmodium falciparum*, consisting of three NANP repeats. Modeling of the insertion in the milieu of the YF 17D virus E protein suggested that it could adopt several conformations without significantly interfering with the overall E protein structure (1). A recombinant virus (YF 17D/8) expressing this insertion flanked by two glycine residues at each end is specifically neutralized by a monoclonal antibody to the model epitope. Furthermore, mouse antibodies raised against the recombinant virus recognize the parasite protein in an enzyme-linked immunosorbent assay (ELISA). Serial passage analysis confirmed the genetic stability of the insertion in the viral genome.

The attenuation of YF 17D virus for humans must be veri-

* Corresponding author. Mailing address: Departamento de Bioquimica e Biologia Molecular, Fundação Oswaldo Cruz., Avenida Brasil 4365, Manguinhos, Rio de Janeiro, RJ, Brazil, 21040-900. Phone: 55 21 3865 8112. Fax: 55 21 2590 3495. E-mail: rgaller@ioc.fiocruz.br.

fied by a highly standardized neurovirulence test in nonhuman primates (12, 30) This test has been used to study the attenuation of several recombinant and nonrecombinant YF 17D viruses (5, 7, 8, 12, 15, 16). Here, we have used the internationally accepted MNVT to show that the insertion of two protein epitopes, of different amino acid sequences and lengths, into the E protein at the *fg* loop did not alter the attenuation of the respective recombinant YF 17D viruses.

## MATERIALS AND METHODS

**Modeling of the YF 17D virus E protein.** We have previously described a sequence alignment of several different flavivirus E proteins and its application in the construction of homology models for the YF virus envelope protein and in the identification of insertion sites therein for the expression of heterologous peptide epitopes (1). Based on this alignment, 10 models were built for a dimer of the YF virus E protein carrying the nonapeptide $CD8^+$ epitope SYVPSAEQI, derived from the CS protein of the rodent parasite *Plasmodium yoelii*. Models were built by the satisfaction of spatial restraints as implemented in the MODELLER program (25), based on the known crystal structure of the neutral-pH (dimeric) form of the E protein from tick-borne encephalitis (TBE) virus (22). For each model, a default coordinate randomization in Cartesian space of 4 Å was employed, prior to model optimization using the variable target function method followed by simulated annealing. The nine-residue insert was modeled into the *fg* loop between residues E199 and T200 of the YF virus E protein sequence. Deliberate misalignment of the first and final residues of each insertion/deletion in the sequence alignment was used in order to relax the homology constraints and facilitate achieving acceptable stereochemistry in the region. A similar approach was taken to the modeling of the YF 17D virus E protein carrying no heterologous peptide.

Ten models carrying the insert $GG(NANP)_3GG$ in the same site were generated as described previously (1). In this case the threefold NANP repeat, derived from the human parasite *Plasmodium falciparum* CS protein, was flanked by two glycine spacers on either side in order to better accommodate the insert in the *fg* loop and to render it more accessible.

The resulting models were evaluated initially via their pseudo-energies [$-\ln(P)$, where P is the MODELLER molecular probability function including both homology-derived and stereochemical terms] and subsequently by using the PROCHECK (11), VERIFY_3D (13), and WHATIF (29) programs for the analysis of model stereochemistry, residue environments, and atomic contacts, respectively. During this process particular attention was paid to the inserted residues and their vicinity. Analysis of the best models concentrated on both structural and functional aspects of the molecule and included comparisons with the recently described low-pH (trimeric) form of the E proteins from TBE and dengue viruses (2, 18).

**Cell cultures.** Vero cells, originally obtained from the American Type Culture Collection, were grown in 199 medium supplemented with 5% fetal bovine serum.

**Construction of infectious cDNA clones.** The regeneration of YF 17D virus from cDNA was first described by Rice et al. (23). Here, two plasmids containing different portions of the YF virus genome were joined to assemble the complete genome from which infectious RNA can be transcribed. For the insertions at the *fg* loop, an EcoRV site was created at nucleotide 1568 of the viral genome in plasmid pYF5′3′IV (1, 23). The resulting plasmid was called pYFE200. By cutting pYFE200 and pT3/27 (a derivative of pYFM5.2) with NsiI/SalI, specific restriction fragments were generated which, upon ligation, reconstituted the complete YF virus genome in the cDNA form. Linearization of this cDNA with XhoI allows its use for in vitro synthesis of viral RNA. The construction of full-length clones with the insertion of the humoral epitope $(NANP)_3$ was described by Bonaldo et al. (1), and the virus regenerated from this plasmid was named YF 17D/8. For the regeneration of a virus expressing the *P. yoelii* CS protein $CD8^+$ epitope (SYVPSAEQI), the corresponding oligonucleotides, with the codon usage of the YF genome, were inserted into the EcoRV site of plasmid pYFE200. This plasmid was used for template preparation and in vitro transcription as described elsewhere (1, 23).

**Recovery of virus from cloned cDNA: transcription and transfection.** The in vitro-ligated template resulting from pYFE200 containing the SYVPSAEQI epitope with the pT3/27 plasmid system and full-length pYF17D/MAL8 were transcribed by SP6 RNA polymerase (AmpliScribe SP6; Epicentre Technologies), and the RNAs were transfected with Lipofectamine (GIBCO BRL), as previously described (3). The recovered viruses were named YF 17D/13 and YF 17D/8, respectively.

**Viral stocks, viral growth, and plaque size characterization.** Following transfection, viruses were harvested after the onset of the cytopathic effect, and titers were determined by plaque assay on Vero cells. Viral stocks were prepared by infecting Vero cell monolayers with posttransfection supernatants at a multiplicity of infection (MOI) of 0.1. These second-passage stocks were titered and were used in all steps of virus characterization. Viral growth curves were determined by infecting monolayers of Vero cells at an MOI of 0.02. Cells were plated at a density of 62,500/$cm^2$ and infected 24 h later. Samples of cell culture supernatants were collected at 24-h intervals postinfection. Viral yields were estimated by plaque titration on Vero cells at a density of 50,000/$cm^2$ with 3.5% carboxymethylcellulose as an overlay. Determination of the plaque size was made by growing viruses in Vero cells plated at 62,500/$cm^2$ in six-well plates with a 3-ml overlay of 0.5% low-melting-point agarose in 199 medium supplemented with 5% fetal bovine serum. Following 4 days of incubation at 37°C, 2.0 ml of medium supplemented with 0.1% neutral red was added, and the plates were incubated for 1 day prior to fixation in 10% formaldehyde and subsequently stained with 0.01% crystal violet.

**Reverse transcription-PCR (RT-PCR) and sequencing.** Recombinant 17D/8 and 17D13 virus stocks corresponding to the third passage in Vero cell monolayers were used to initiate the additional 10 serial passages in all animal experiments and for complete-genome sequencing. Viral suspensions were used for RNA extraction with Trizol LS (Invitrogen, Life Technologies), and RNA was precipitated with isopropanol in the presence of glycogen (Invitrogen, Life Technologies). The RNA was used as a template for cDNA synthesis with a negative-strand YF virus-specific synthetic, followed by PCR amplification with the GeneAmp 9600 instrument (Applied Biosystems) and the GeneAmp RNA PCR Core kit (Applied Biosystems). The analysis of insert genetic stability was based on the sequencing of a limited genomic region (nucleotides 1131 to 1781) encompassing the *fg* loop area in the E protein gene. This was done using RNA extracted from the YF 17D/8 and 17D/13 viruses at their fifth and tenth serial passages in Vero cells and also for viruses corresponding to the transfection supernatant and its first passage in Vero cells.

For complete genomic sequence determination carried out on viral stocks used in animal experimentation (third passage), amplification of viral genomic regions was performed essentially as described elsewhere (5). A total of 11 RT-PCR fragments were designed comprising nucleotides 1 to 1066, 940 to 1799, 1641 to 2639, 2361 to 3387, 3004 to 4286, 4181 to 5071, 4980 to 6325, 6102 to 7272, 7162 to 8420, 8302 to 9586, and 9425 to 10862; within these fragments, internal primers were positioned on both cDNA strands for the overlapping sequencing reactions. Nucleotides were numbered, and primers were designed, according to the YF 17D vaccine strain sequence (GenBank accession number X03700). Amplification products were further purified from excess primers with silica-based purification kits (QIAGEN). The purified products were sequenced directly without molecular cloning. Nucleotide sequencing reactions were performed with the BigDye terminator mix, version 2.0 (Applied Biosystems), according to the manufacturer's recommendations. Electrophoresis of fluorescent products was performed in an ABI PRISM 3100 instrument (Applied Biosystems). Nucleotide sequences were analyzed using Chromas software, version 1.45 (Technelysium), and a consensus sequence for each viral genome was derived from contiguous sequences using SeqMan II software from the Lasergene package, version 4.05 (DNAStar).

**Genetic stability assay.** Recombinant viruses were serially passaged in Vero cells at an MOI of 0.02. For the supernatants of the fifth and tenth passages, viral suspensions were extracted with Trizol LS, and cDNA was synthesized and sequenced as described above.

**Experimental inoculation of rhesus monkeys.** Studies were carried out using a protocol reviewed and approved by the Institutional Committee for Experimentation and Care of Research Animals (CEUA-Fiocruz, P0112/02).

Four groups of 10 captive-bred healthy rhesus monkeys (*Macaca mulatta*; 26 males and 14 females, weighing 2,980 g to 5,920 g) were obtained from the Primatology Department (CECAL/Fiocruz, Rio de Janeiro, Brazil). Each animal was kept in a separate cage under controlled environmental conditions (temperature, 20 to 22°C; relative humidity, about 60%; 12 h of artificial light and 12 h of darkness). Animals were fed twice daily with monkey chow supplemented with fresh fruits and were allowed water ad libitum. All monkeys were shown to be free of YF virus neutralizing antibodies by a plaque reduction neutralization assay. Virus inoculation, viremia, clinical observation, necropsy, and histological examination have been described previously (5, 15).

The viral inocula were back titrated by a plaque assay on Vero cells. Doses of the YF secondary seed lot virus (YFV 17DD 13Z) were 26,303 mouse 50% lethal doses ($LD_{50}$) in experiment I and 33,884 mouse $LD_{50}$ in experiment II. The

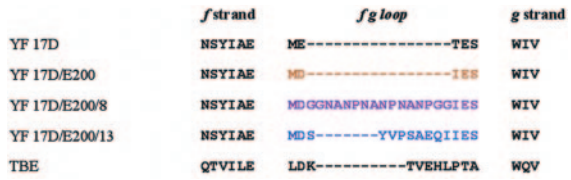


FIG. 1. Amino acid sequences of the *fg* loops of different flaviviruses. The amino acid sequences at the regions comprising parts of the *f* and *g* strands and at the *fg* loops of the different YF viruses (17D-204 strain sequence, GenBank accession number X15062), and the homologous regions of TBE virus E protein (Neudoerfl strain, GenBank accession number U27495), were aligned using Clustal W.

intracerebral (i.c.) dose of the YF 17D/8 virus was 26,303 mouse $LD_{50}$, whereas that of the YF 17D/13 virus was 10,471 mouse $LD_{50}$.

Seroconversion to YF was determined by the plaque reduction neutralization test at a 50% end point (15, 26). Results were expressed in thousandths of international units per milliliter (mIU/ml), using an international reference serum preparation for yellow fever containing 14,300 mIU/ml (World Health Organization [WHO], International Biological Standard, held by Statens Serum Institut, Copenhagen, Denmark; International Reference Preparation of Anti-Yellow-Fever Serum, 14.3 IU/vial, lot identification YF XIII-125 1000 6 62). Although this unit system is not frequently used in the literature to express YF virus neutralizing antibody titers, we provide the data in this format so that our results can readily be compared with those from other laboratories using a standardized unit system. The reciprocal of the dilution at the 50% plaque reduction end point of the reference preparation corresponds to 14,300 mIU/ml. This reference preparation was used to calibrate an in-house standard monkey serum by using both in parallel neutralization assays. The amount of mIU/ml for the in-house standard was calculated by the formula (reciprocal of the dilution at 50% for the in-house serum × 14,300)/(reciprocal of the dilution at 50% for the reference preparation). The in-house standard was included in all neutralization assays performed to obtain the data shown in Table 1 by using the formula (reciprocal of the dilution at 50% for the test serum) × (in-house titer in mIU/ml)/(reciprocal of the dilution at 50% for the in-house standard). Antibodies to the NANP repeat epitope were detected by ELISA as described elsewhere (1) but using microtiter plates (Costar, Cambridge, MA) coated with 50 ng/well of the resin multiple antigen peptide (MAP) containing the three-repeat B-cell epitope of the CS protein of *P. falciparum* [MAP-$(NANP)_3$].

**Statistical analysis.** Means and standard deviations were calculated for clinical and combined histological scores. The Student *t* test was used for comparing means. When there was a suggestion that the data were asymmetrical or that variances were not homogeneous, the Kruskal-Wallis nonparametric test was performed. Differences were considered statistically significant if the *P* value was 0.05 or less. Statistical analyses were done using Stata 7.0 software (Stata Corp., College Station, Tex., 2002).

## RESULTS

**Comparative analysis of the three-dimensional (3D) structures of the E proteins from the YF 17D/8 and 17D/13 viruses.** We have previously shown that a repetitive humoral epitope of the parasite *Plasmodium falciparum* was stably cloned and expressed at the *fg* loop of the 17D virus E protein (1). We wanted to validate the usefulness of this site for the expression of a variety of epitopes with other immunological specificities. For this purpose we selected a second *Plasmodium* epitope that has been shown to be involved in the protection of mice against challenge with the *Plasmodium yoelii* $CD8^+$ T-cell epitope SYVPSAEQI (28).

The *fg* loop chosen as the insertion site is variable in length between flaviviruses; it is six residues longer in TBE virus than in YF virus (Fig. 1). Upon introduction of the nine-residue SYVPSAEQI epitope into this loop, the resulting structure is therefore only three residues longer than that observed in TBE virus. Furthermore, there is a reasonable degree of sequence similarity between the C terminus of the original TBE virus loop (sequence EHL) and that of the insert (EQI). Taken together, these observations suggested that this insert might be tolerated within the *fg* loop without further alterations. This speculation is borne out by quality analysis of the best overall model, which presented a PROCHECK G-factor of 0.07 (equivalent to a crystal structure at <1.0 Å resolution) with 92% of the residues in the most favorable regions of the Ramachandran plot and no stereochemical distortions in the region of the insertion sites in the two monomers. Furthermore, the overall WHATIF atomic contact quality for this model was −1.0 and the VERIFY_3D score was 350 (compared to an expected value of 369 for a protein of the same length), both indicating the model to be reliable in terms of overall packing. More importantly, one of the inserts of the dimer had a local average VERIFY_3D environment score for the *fg* loop of 0.34/residue. This is above that observed for the crystal structure of the E protein from TBE virus, on the basis of which the model was built (0.28/residue). Overall the modeling results therefore suggest that it is possible to accommodate the insert in the *fg* loop of the dimer while preserving reasonable chemical environments for the additional residues (Fig. 2).

We have described previously the models for the $GG(NANP)_3GG$ sequence inserted into the YF 17D virus E protein and the rationale behind the inclusion of the glycine spacers in this case (1). Principally, this was based on the expected need to leave this B-cell epitope exposed on the viral surface while minimizing the size of the spacers. A second reason was that, in contrast to the T-cell epitope described above, there was a complete lack of any sequence similarity between the $(NANP)_3$ epitope and the original sequence for the *fg* loop in TBE virus.

Models of the 17D/8 insert show that the effect of the glycine spacers is to lift the $(NANP)_3$ epitope above the surface of the virus, making it more solvent exposed (1) (Fig. 2A and B). Although there is a great diversity of conformations for the insert among the models, some common features are still discernible. Analysis of the 20 loops corresponding to the 10 dimeric models shows that they rarely contribute significantly to the dimer interface and that they present an average increase in the intermonomer contact surface of only 57 $Å^2$, compared with the 217 $Å^2$ observed for the 17D/13 virus. Furthermore, in many of the models, the two salt bridges seen in many of the 17D virus E protein structures are also conserved (Fig. 2C). Overall, there is little indication that this loop would significantly alter dimer stability.

It is of interest to examine the potential impact of the inserted epitopes on functional aspects of the structure of the E protein, including the potential occlusion of residues believed to participate in the receptor binding surface of domain III, the stabilization or destabilization of the dimer interface, and the compatibility of the insert with the trimeric form of the structure, which is a prerequisite for host cell invasion.

In the case of the 17D/13 nonapeptide insert, the majority of the models show the *fg* loop rising from a hollow in the molecule and projecting only slightly from its external surface (Fig. 2A and B). Because this loop is only slightly larger than the original TBE virus loop of six residues, it occupies a similar volume of space and cannot reach either the fusion peptide or the receptor binding surface of domain III on either of the two

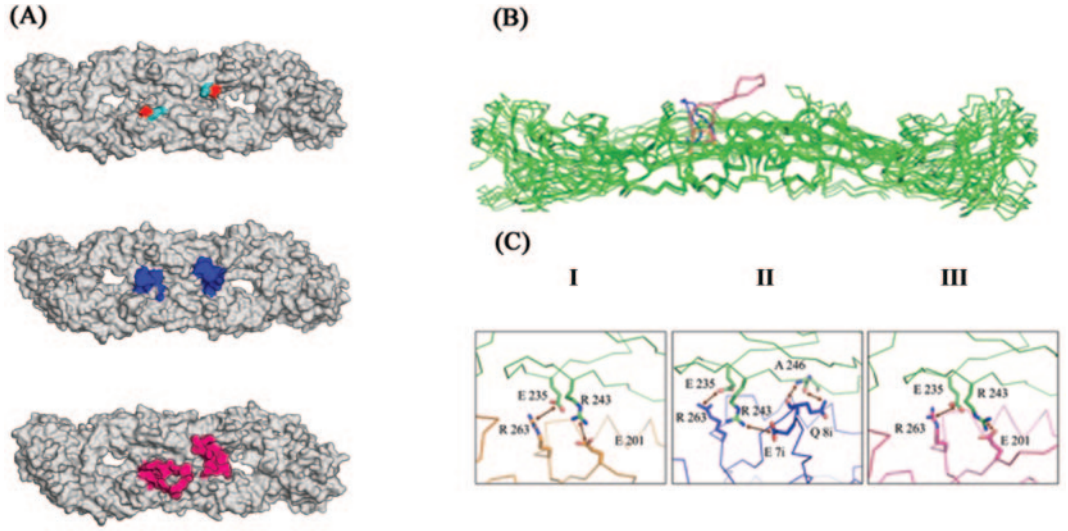


FIG. 2. 3D models of the YF 17D vaccine virus and recombinant E proteins. (A) Surface representations of typical models for the YF 17D (I), 17D/13 (II), and 17D/8 (III) viruses. In model I, the N and C termini of the insert site are indicated in light blue and red, respectively. In models II and III, the molecular surface of the insert is highlighted in dark blue (17D/13) or pink (17D/8). (B) Superposed Cα trace for the three models highlighting the insertion site by following the same color scheme (wild type in orange). The remainder of the molecule, together with the original TBE crystal structure, is shown in green. In the YF 17D virus, the *fg* loop is buried in a hollow on the molecular surface from which the inserts project. (C) Potential salt bridges and hydrogen bonds across the dimer interface. In all cases, the upper subunit is shown in green and the lower subunit is shown according to the color scheme used in subsequent figures. Models for (I) the YF 17D virus (orange) showing two potential salt bridges, (II) the 17D/13 virus (blue), in which hydrogen bonds involving a glutamine residue within the insert are observed in addition to the two salt bridges, and (III) the 17D/8 virus (pink), which is essentially identical to the wild type. Numbering is shown according to the YF 17D sequence, and residues within the insert are indicated by a lowercase "i." Interactions shown by yellow arrows summarize typical results for the 10 models, but due to considerable variation between them, they are not necessarily observed in all structures.

monomers. This observation is also valid for the 17D/8 insert, despite its additional size.

An increase in monomer-monomer contact is observed in all cases compared with models for the YF 17D virus E molecule. This leads to a total mean solvent-inaccessible contact area of 1,460 $Å^2$ for the models, which is comparable to the 1,503 $Å^2$ observed for TBE virus and 217 $Å^2$ greater than that observed for models of the YF 17D virus E protein. Overall, this increase in contact area across the dimer interface, part of which is due to specific hydrogen bond interactions, would be expected to increase the stability of the dimer.

At least two salt bridges can potentially form across the dimer interface of YF 17D/13 virus E protein (Fig. 2C). These were also observed in models for the YF 17D virus E protein, although in some cases a glutamate from the insert itself (E7i) performed the role played by E201 in the original sequence (Fig. 2C). Furthermore, many of the models show the formation of a hydrogen bond between the penultimate glutamine residue of the insert (Q8) and the main chain of the neighboring monomer (in the model shown in Fig. 2, this is via A246). The details of these interactions vary from one model to another and are the consequence of the inherent uncertainties in homology modeling of loop insertions.

The interdomain interfaces of the E protein appear to be critical for protein functionality, as reorientation of the domains is the principal conformational change to occur during the dimer-to-trimer transition. Particularly relevant in the present context is the observed flexibility of the *kl* loop, which lies adjacent to the *fg* loop at the interface between domains I and II (2, 17, 18). In the 10 models for the 17D/13 insert, there is an observed correlation between the conformations of the two loops, indicating that the insert has potential structural and functional consequences for the region. For the 17D/8 virus no such correlation is observed, most probably due to the presence of the glycine spacers which flank the epitope itself. In the final postfusion trimer, the *fg* loop is located about halfway up the lateral surface of the elongated molecule in a manner similar to that seen in the dimer on which it was built (Fig. 3). Thus, although the trimeric structure was unknown at the time when the inserts were designed, the use of the *fg* loop appears to be compatible, at least in structural terms, with both oligomeric forms.

**Construction and characterization of a recombinant YF 17D virus expressing a *P. yoelii* CS T-cell epitope.** As predicted from the 3D structure analysis, there was expected to be no need to add the glycine spacers for the insertion of the $CD8^+$ T-cell epitope SYVPSAEQI into the YF 17D virus E protein *fg* loop, as was done previously for the cloning of the humoral epitope.

The resulting virus, YF 17D/13 virus, after two passages in Vero cells, led to viral stocks that had titers of 6.62 $\log_{10}$ PFU/ml. The presence of the insert in the viral genome was confirmed by sequencing of the cDNAs made from the viruses

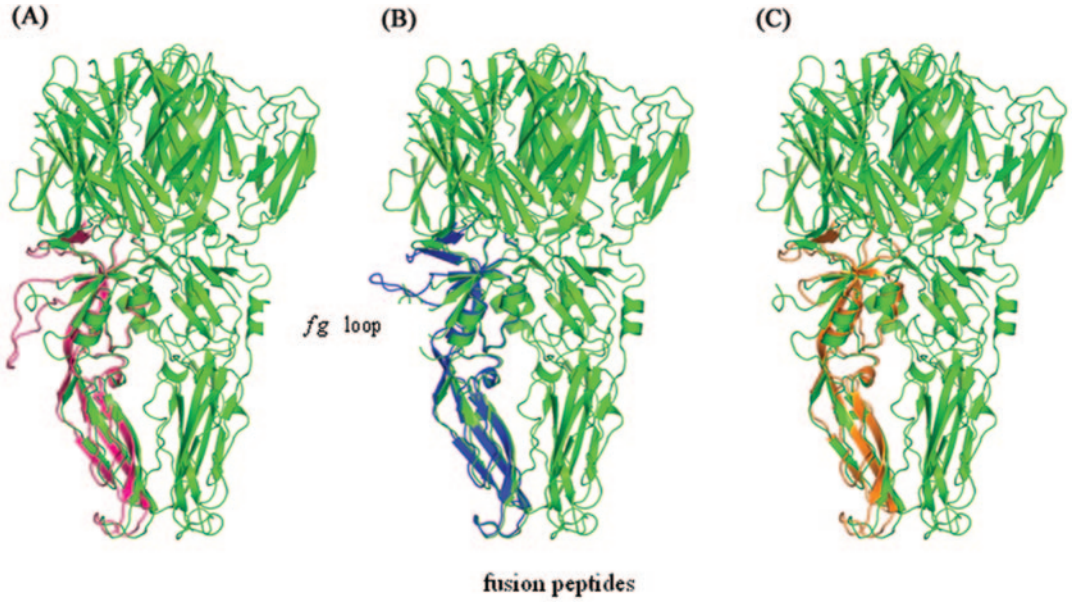


FIG. 3. Superposition of domain II from each model onto the same region from one of the monomers of the low-pH trimeric form of the TBE virus E protein (green). (A) The 17D virus (orange) has a smaller *fg* loop than that seen in TBE virus, which is variably disordered in the crystal structure. (B) The 17D/13 virus (blue), showing an *fg* loop comparable in size to that of TBE virus. (C) The 17D/8 virus (pink), showing how the large *fg* insert projects from the trimer surface and would potentially interfere with the association of trimers during membrane fusion. For clarity, the *fg* loop and the clustering of the fusion peptides at the bottom tip of the molecule are indicated only in the central image.

present in the cell culture supernatants derived from both stocks, after transfection and a second passage in Vero cells.

Based on single-step growth curves in Vero cells, differences were observed between the insertion-bearing viruses and control viruses (Fig. 4). Both recombinant viruses produced peak titers at 96 h postinfection, like the control 17D/E200 virus but in contrast to the 17DD virus, which exhibited a peak titer at 72 h postinfection. However, the 17D/8 virus peak titer was nearly six- and twofold lower than those of the 17DD and 17D/E200 control viruses, respectively. The 17D/13 virus showed a reduction in peak titer of almost twofold compared to that of the 17DD control virus but no significant difference from that of 17D/E200.

In Vero cells, both recombinant viruses produced tiny plaques, 1.10 ± 0.26 mm for 17D/8 virus and 1.51 ± 0.28 mm for 17D/13, compared to the 17DD virus (5.3 ± 1.4 mm) and the small-plaque 17D/E200 virus (3.2 ± 0.9 mm).

**Recombinant virus attenuation for rhesus monkeys.** The definition of the attenuation of YF viruses must come from an internationally accepted MNVT, as recommended by WHO for the characterization of new YF seed and vaccine viruses (30). Here, quantitative histopathological examination of brain and spinal cord tissue provides a sensitive method for distinguishing strains of the same virus with subtle differences in neurovirulence (12, 15, 16).

We examined the attenuation of the YF 17D/13 and 17D/8 viruses by the current monkey neurovirulence test (30) in order to address specific preclinical safety concerns. For this purpose we performed two separate tests to check the phenotypes of the two different recombinant viruses. In each test, a group of 10 monkeys was inoculated with the known vaccine control as recommended (30)—in our case, the 17DD virus–and another 10 animals received the experimental virus.

**Viremia.** Table 1 displays the data on viremia recorded for monkeys inoculated with each virus. Mean peak viremia was calculated based on the peak value for each monkey in a given group. Monkeys for whom viremia was undetectable by plaquing on Vero cells at a low dilution (dilution, 1:3; titer, $<0.6$ $\log_{10}$ PFU/ml) were given a titer of zero in the calculation. Because the serum samples from monkeys in group IV were negative by plaquing, cultivation, and RT-PCR, determination of the absence of virus in sera from animals belonging to other groups was based only on plaquing. However, attempts to detect viral RNA by RT-PCR in sera from other MNVTs with 17DD virus failed to reveal any positives not detected by plaquing. Therefore, assuming the zero for the calculation of mean titers was a reasonable alternative to include all monkeys.

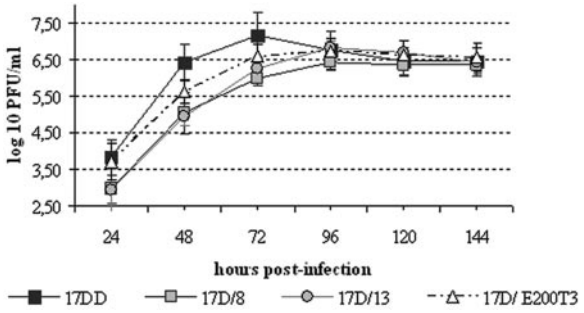


FIG. 4. YF 17D virus growth in Vero cells. Monolayers of Vero cells were infected either with control virus 17DD (black squares) or 17D/E200T3 (open triangles) or with a recombinant virus (17D/13 [gray circles] or 17D/8 [gray squares]) at an MOI of 0.02. Values at each time point represent the average titer obtained from three separate experiments with the respective standard deviations.

TABLE 1. Viremia in rhesus monkeys inoculated by the intracerebral route with YF 17D viruses

| Virus | Monkey | Viremia[a] | | | | | Total days of viremia[b] |
|---|---|---|---|---|---|---|---|
| | | Day 2 | Day 4 | Day 6 | Mean peak titer (SD) | Range | |
| 17DD (group I) | 114 | <0.6 | **1.83** | <0.6 | 1.09 (0.77) | 0–2.42 | 10 |
| | 116 | **0.6** | <0.6 | <0.6 | | | |
| | 159 | <0.6 | <0.6 | **1.08** | | | |
| | 162 | **1.20** | **1.20** | <0.6 | | | |
| | 240 | **1.68** | <0.6 | <0.6 | | | |
| | 303 | <0.6 | <0.6 | <0.6 | | | |
| | 810 | **0.9** | **2.42** | <0.6 | | | |
| | 934 | <0.6 | <0.6 | <0.6 | | | |
| | 4U | <0.6 | **1.20** | <0.6 | | | |
| | O31 | <0.6 | 0.9 | <0.6 | | | |
| 17D/13[c] (group II) | 178 | <0.6 | **0.6** | <0.6 | 0.44 (0.52) | 0–1.44 | 5 |
| | 253 | <0.6 | **1.44** | <0.6 | | | |
| | 423 | <0.6 | **0.6** | <0.6 | | | |
| | 520 | <0.6 | **0.9** | <0.6 | | | |
| | 540 | <0.6 | <0.6 | <0.6 | | | |
| | 558 | <0.6 | **0.90** | <0.6 | | | |
| | 4A | <0.6 | <0.6 | <0.6 | | | |
| | 6U | <0.6 | <0.6 | <0.6 | | | |
| | 46 | <0.6 | <0.6 | <0.6 | | | |
| | T73 | <0.6 | <0.6 | <0.6 | | | |
| 17DD (group III) | T21 | **1.08** | <0.6 | <0.6 | 0.99 (0.33) | 0–1.55 | 14 |
| | T23 | **0.6** | <0.6 | <0.6 | | | |
| | T25 | <0.6 | <0.6 | **0.6** | | | |
| | T45 | **0.9** | **0.9** | <0.6 | | | |
| | T57 | 0.6 | <0.6 | <0.6 | | | |
| | T77 | <0.6 | **1.2** | **1.3** | | | |
| | T81 | <0.6 | **0.9** | <0.6 | | | |
| | U11 | **1.3** | <0.6 | <0.6 | | | |
| | U41 | **0.9** | **1.55** | <0.6 | | | |
| | U71 | **0.9** | **1.08** | <0.6 | | | |
| 17D/8[c] (group IV) | T17 | <0.6 | <0.6 | <0.6 | 0 | 0 | 0 |
| | T19 | <0.6 | <0.6 | <0.6 | | | |
| | T43 | <0.6 | <0.6 | <0.6 | | | |
| | T49 | <0.6 | <0.6 | <0.6 | | | |
| | T51 | <0.6 | <0.6 | <0.6 | | | |
| | T63 | <0.6 | <0.6 | <0.6 | | | |
| | T65 | <0.6 | <0.6 | <0.6 | | | |
| | T69 | <0.6 | <0.6 | <0.6 | | | |
| | U5 | <0.6 | <0.6 | <0.6 | | | |
| | U49 | <0.6 | <0.6 | <0.6 | | | |

[a] Expressed as $\log_{10}$ PFU per milliliter. Values for detectable viremia are boldfaced. *P* values for differences in mean peak titer between groups were as follows: for group I versus II, $P = 0.04$; for group I versus III, $P = 0.71$; for group II versus IV, $P = 0.01$; and for group III versus IV, $P < 0.001$.

[b] *P* values for differences in duration of viremia between groups were as follows: for group I versus II, $P = 0.08$; for group I versus III, $P = 0.15$; for group II versus IV, $P = 0.008$; for group III versus IV, $P < 0.001$.

[c] Viral stocks were used at the third passage level.

In the experimental infection of rhesus monkeys by the i.c. route with the 17DD and 17D/13 viruses (groups I and II, respectively), monkey serum viremia differed between the two groups: only 5 animals were viremic at any given day (day 2, 4, or 6) after inoculation with the 17D/13 virus, while 17DD induced viremia in 8 out of 10 animals. Viremia was most prevalent in both groups at the fourth day postinfection, when 5 out of 10 monkeys showed measurable circulating virus. Monkeys that received the 17D/13 virus had detectable viremia in 5 out 30 measured points (10 monkey sera tested on each of days 2, 4, and 6), whereas the 17DD group had viremia in 10 out of 30. The mean peak viremia for the 17D/13 virus was 0.44 $\log_{10}$ PFU/ml (range, 0 to 1.44), whereas for 17DD it was significantly higher (1.09 $\log_{10}$ PFU/ml; range, 0 to 2.42) ($P = 0.04$ by the *t* test).

Groups III and IV, which received the 17DD and 17D/8 viruses, respectively, also showed limited viremia. The 17DD virus induced viremia in all animals of group III for a total of 14 days and at a mean peak titer of 0.99 $\log_{10}$ PFU/ml (range, 0 to 1.55), whereas no viremia at all was detected for the YF 17D/8 virus ($P < 0.001$ by the *t* test). Viremia was not significantly different between the two groups that received the control 17DD virus in terms of mean peak titer ($P = 0.71$ by the *t* test) or duration ($P = 0.15$ by the *t* test). Animals inoculated with the 17D/13 virus (group II) showed a significantly higher mean peak titer of viremia as well as a significantly greater duration than monkeys in group IV ($P = 0.01$ and $P = 0.04$, respectively, by the *t* test).

Serum samples from all 10 animals that received the 17D/8 virus were also inoculated into flasks of Vero cell cultures and

TABLE 2. Antibody response to YF virus inoculation

| Virus | Monkey | Titer of antibody to YF virus (mIU/ml)[a] | | Titer of antibody to NANP[b] | |
|---|---|---|---|---|---|
| | | Preinoculation | Postinoculation | Preinoculation | Postinoculation |
| 17DD (group I) | 114 | <447 | 95,471 | NA | NA |
| | 116 | <447 | 30,124 | NA | NA |
| | 159 | <447 | 41,210 | NA | NA |
| | 162 | <447 | 35,872 | NA | NA |
| | 240 | <447 | >100,000 | NA | NA |
| | 303 | <174 | 46,773 | NA | NA |
| | 810 | <174 | 72,028 | NA | NA |
| | 934 | <100 | >100,000 | NA | NA |
| | 4U | <100 | >100,000 | NA | NA |
| | O31 | <100 | 16,999 | NA | NA |
| 17D/13[c] (group II) | 178 | <447 | 50,646 | NA | NA |
| | 253 | <174 | 37,770 | NA | NA |
| | 423 | <174 | 32,393 | NA | NA |
| | 520 | <174 | 13,375 | NA | NA |
| | 540 | <174 | 8,511 | NA | NA |
| | 558 | <174 | 646 | NA | NA |
| | 4A | <100 | 40,179 | NA | NA |
| | 6U | <100 | 10,448 | NA | NA |
| | 46 | <100 | 7,154 | NA | NA |
| | T73 | <100 | 1,136 | NA | NA |
| 17DD (group III) | T21 | <347 | >100,000 | 0 | 0 |
| | T23 | <347 | 46,130 | 0 | 0 |
| | T25 | NT | NT | | |
| | T45 | <316 | >100,000 | 0 | 0 |
| | T57 | <234 | 91,687 | 0 | 0 |
| | T77 | <316 | 33,374 | 0 | 0 |
| | T81 | <316 | 29,677 | 0 | 0 |
| | U11 | <550 | 69,631 | 0 | 0 |
| | U41 | <550 | 67,805 | 0 | 0 |
| | U71 | <550 | 32,359 | 0 | 0 |
| 17D/8[c] (group IV) | T17 | <347 | 946 | 0 | 40 |
| | T19 | <347 | 3,654 | 0 | 1,280 |
| | T43 | <347 | 355 | 0 | 160 |
| | T49 | <234 | 792 | 0 | 160 |
| | T51 | <234 | 3,876 | 0 | 160 |
| | T63 | <234 | 13,964 | 0 | 320 |
| | T65 | <234 | 1,166 | 0 | 160 |
| | T69 | <316 | <316 | 0 | 40 |
| | U5 | <316 | 776 | 0 | 160 |
| | U49 | <550 | 8,318 | 0 | 160 |

[a] Determined by the plaque reduction neutralization test at a 50% end point. NT, not tested.
[b] Determined by an ELISA for $(NANP)_3$. Each serum sample was serially diluted from 1:20 to 1:2,560; each titer is expressed as the reciprocal of the highest serum dilution that presented an $A_{492}$ of >0.1. NA, not applicable.
[c] Viral stocks at third passage level.

incubated for 1 week, with no evidence of cytopathic effect. These cultures were then split and incubated for another week without evidence of viral growth. RT-PCR analysis performed directly on monkey sera also failed to reveal the presence of the viral genome. Because we followed the recommended WHO protocol, samples were not taken after the sixth day, and therefore it remains unknown whether the 17D/8 virus crosses the blood-brain barrier to reach the peripheral blood after this period.

The onset of fever in animals inoculated with the 17D/8 virus occurred at 10.5 days (standard deviation [SD], 1.8), compared to 8 days (SD, 0.81) for animals that received the 17DD virus. This late onset may reflect virus circulation after the sixth day postinfection. It has been shown (15) for the YF 17DD virus that fever is preceded by viremia, and there was no detectable 17D/8 viremia until the sixth day. Since the onset of fever for the 17D/8 virus occurred later than that observed for 17DD, there might have been virus circulation after the sixth day postinoculation.

**Seroconversion.** All animals developed neutralizing antibodies 30 days after YF virus inoculation, as indicated by plaque reduction neutralization tests, with the exception of monkey T69, inoculated with the YF 17D/8 virus (Table 2). However, this monkey had detectable antibody to the foreign epitope at a 1:40 dilution, whereas all nine other animals that received the same virus had titers ranging from 1:40 to 1:1,280 (reciprocal of the dilution).

Neutralizing antibody titers to YF virus ranged from 355 to more than 100,000 mIU/ml. It must be pointed out that a total of five neutralization titers went off scale (>100,000; monkeys

240, 934, and 4U in group I, and monkeys T21 and T45 in group III [Table 2]). Therefore, the means could not be calculated. In order to compare the test groups, we used their medians, since this measure, in our case, was not affected by the extreme values, including those off scale. To compare the medians, we employed a nonparametric test that uses ranks, the Kruskal-Wallis test. The YF 17DD virus was significantly more immunogenic by the intracerebral route than the YF 17D/13 virus ($P = 0.0051$) or the 17D/8 virus ($P = 0.0002$). No statistical significance was observed for the difference in antibody titer between the two groups of animals inoculated with the 17DD virus, whereas 17D/13 was significantly more immunogenic than 17D/8 ($P = 0.02$).

**Clinical score.** Table 3 displays the individual clinical scores after the 30-day observation period for both neurovirulence tests. This score is the average of the values given at each day during this period for each monkey. For the first experiment, comparing our 17DD vaccine virus and the 17D/13 recombinant, the results show (Table 3) that only two monkeys (monkeys 6U and 46) inoculated with the 17D/13 virus displayed any clinical signs, compared to five monkeys inoculated with the 17DD virus (monkeys 114, 240, 303, 810, and O31). The fact that several animals displayed viremia and all specifically seroconverted to YF confirms that the animals were indeed infected by the inoculated viruses. Monkeys 114, 240, and 810, inoculated with the 17DD virus, had the highest viremias but minimal clinical scores (0.07, 0.14, and 0.64, respectively). For 17D/13, monkey 253 showed no clinical signs and had the highest viremia in the group (Tables 1 and 3). The overall clinical score for each group is given in Table 3 along with the histological scores. The mean clinical score for the YF 17DD vaccine virus was 0.11, whereas that for 17D/13 was 0.16. Since the values do not show a homogeneous distribution, we used a nonparametric statistical test to analyze the significance of the difference between the two means. According to the Kruskal-Wallis test, this difference was not significant ($P = 0.37$).

A somewhat higher score for the 17D/13 virus was due to a single outlier monkey (6U) that presented signs of encephalitis such as slow and incomplete movements, as well as tremors, that lasted for 10 days. This particular monkey showed no viremia, did seroconvert to YF, and did not present histological alterations in the central nervous system (CNS) compatible with the clinical picture (Table 3). It showed a low target area score (1.0); the nucleus caudatus and putamen were given scores of 0.5 and 0.75, respectively; and the nuclei thalami had values of 0.25. The spinal cord showed no lesions at the cervical level, and at the lumbar, only minor damage (grade 1) could be observed in one hemisection out of the six areas analyzed (score, 0.08). Monkeys 178, 253, 423, 540, T73, 4A, and 46 had higher histological scores for the same areas and yet showed no clinical signs.

In the second experiment, comparing the YF 17DD vaccine virus to the YF 17D/8 recombinant virus, we observed that in the group inoculated with the latter, only 1 monkey (T49) displayed minor clinical signs, compared to 7 out of 10 animals inoculated with 17DD.

Among these seven animals, two (T25 and T45) showed signs of encephalitis starting at days 7 and 8, respectively, after inoculation. Monkey T25 died on day 8 with low-grade fever, whereas monkey T45 showed only 1 day of fever (day 8 postinoculation). Monkey T45 continued with encephalitic signs until day 17, when it died. As a consequence, both animals showed the highest clinical scores in this group (Table 3). Both animals were within the average weight gain for the group when they died and showed minimal viremia (Table 1). Two other animals showed signs of encephalitis after inoculation with the 17DD virus (T81 and U11) that lasted for 2 and 3

TABLE 3. Neurovirulence of YF 17D viruses for rhesus monkeys

| Virus | Monkey | Clinical score[a] | Discriminator area score | Target area score | Combined score[a] |
|---|---|---|---|---|---|
| 17DD (group I) | 114 | 0.07 | 0.7 | 1.5 | 1.10 |
| | 116 | 0 | 0.42 | 1.5 | 0.96 |
| | 159 | 0 | 0.21 | 0.5 | 0.35 |
| | 162 | 0 | 1.03 | 2 | 1.51 |
| | 240 | 0.64 | 0.78 | 2 | 1.39 |
| | 303 | 0.17 | 0.88 | 2 | 1.44 |
| | 810 | 0.14 | 0.76 | 2 | 1.38 |
| | 934 | 0 | 0.64 | 2 | 1.32 |
| | 4U | 0 | 0.91 | 2 | 1.45 |
| | O31 | 0.1 | 0.52 | 2 | 1.26 |
| Mean | | 0.11 | 0.78 | 1.75 | 1.22 |
| 17D/13[b] (group II) | 178 | 0 | 0.59 | 1 | 0.79 |
| | 253 | 0 | 0.23 | 1 | 0.61 |
| | 423 | 0 | 0.38 | 1 | 0.69 |
| | 520 | 0 | 0.69 | 1.5 | 1.09 |
| | 540 | 0 | 0.47 | 1 | 0.73 |
| | 558 | 0 | 0.57 | 2 | 1.28 |
| | 4A | 0 | 0.67 | 2 | 1.33 |
| | 6U | 1 | 0.33 | 1 | 0.67 |
| | 46 | 0.67 | 0.84 | 2 | 1.42 |
| | T73 | 0 | 0.54 | 1.5 | 1.02 |
| Mean | | 0.16 | 0.53 | 1.40 | 0.96 |
| 17DD (group III) | T21 | 0.6 | 1.12 | 1.50 | 1.31 |
| | T23 | 0.14 | 0.87 | 2.00 | 1.43 |
| | T25 | 3.07 | 1.07 | 2.00 | 1.53 |
| | T45 | 2.77 | 1.62 | 3.00 | 2.31 |
| | T57 | 0.00 | 1.19 | 2.00 | 1.60 |
| | T77 | 0.14 | 1.05 | 1.50 | 1.27 |
| | T81 | 0.40 | 0.87 | 1.50 | 1.18 |
| | U11 | 0.97 | 0.93 | 2.00 | 1.46 |
| | U41 | 0.00 | 0.72 | 2.00 | 1.36 |
| | U71 | 0.00 | 0.81 | 2.00 | 1.40 |
| Mean | | 0.81 | 1.02 | 1.95 | 1.48 |
| 17D/8[b] (group IV) | T17 | 0.00 | 0.67 | 1.00 | 0.83 |
| | T19 | 0.00 | 0.36 | 2.00 | 1.18 |
| | T43 | 0.00 | 0.69 | 2.00 | 1.34 |
| | T49 | 0.50 | 0.81 | 2.00 | 1.40 |
| | T51 | 0.00 | 0.53 | 2.00 | 1.27 |
| | T63 | 0.00 | 1.26 | 2.50 | 1.89 |
| | T65 | 0.00 | 0.61 | 2.00 | 1.30 |
| | T69 | 0.00 | 0.52 | 2.00 | 1.26 |
| | U5 | 0.00 | 0.36 | 1.00 | 0.68 |
| | U49 | 0.00 | 0.75 | 1.50 | 1.12 |
| Mean | | 0.05 | 0.65 | 1.80 | 1.23 |

[a] $P$ values for differences in clinical scores between groups were as follows: for group I versus group II, $P = 0.37$; for group III versus IV, $P = 0.009$; for group I versus III, $P = 0.11$. $P$ values for differences in combined histological scores between groups were as follows: for group I versus group II, $P = 0.05$; for group III versus IV, $P = 0.03$; for group I versus III, $P = 0.15$. $P$ values below 0.05 are considered statistically significant.

[b] Viral stocks at third passage level.

days, respectively, but there was full recovery at the end of the observation period, although with slight weight loss. Both animals showed only 1 day of viremia with minimal titers (Table 1 and 2). The mean clinical score for the 17DD vaccine virus was 0.81, whereas that for 17D/8 was 0.05 (Table 3). As indicated above for the comparison of the clinical scores for the 17DD and 17D/13 viruses, we used a nonparametric statistical test to analyze the significance of the difference between the two means. According to the Kruskal-Wallis test, this difference was found to be significant ($P = 0.009$), and therefore the 17D/8 virus is more attenuated than our YF 17DD vaccine.

The difference in clinical scores between the two groups that received the 17DD virus is noteworthy (Table 3), though not statistically significant ($P = 0.11$ by the Kruskal-Wallis test; if the two outlier monkeys, T25 and T45, are excluded, $P = 0.33$). Marchevsky et al. (15) have shown that for 49 rhesus monkeys inoculated i.c. with the 17DD virus in six different experiments, the mean clinical scores ranged from 0 to 0.57, with heavier animals showing fewer clinical signs. However, the mean weights of the two groups are not disparate (about 700 g), and therefore the observed difference is more likely to be related to test-to-test variation. Moreover, the combined histological scores for the two groups are not significantly different (Table 3; $P = 0.15$ by the Kruskal-Wallis test).

**Histological score.** For all animals, there were no abnormalities in any extraneural organs that could suggest damage or impaired function. None of the animals in either experiment developed any histological lesions of the liver, kidney, adrenals, heart, spleen, or lungs. All 40 rhesus monkeys inoculated i.c with the 17DD, 17D/13, or 17D/8 virus developed histological lesions in the central nervous system (Table 3). As proposed by Levenbook et al. (12), the target area in the rhesus monkey CNS for several vaccine viruses is the substantia nigra. In this study, the substantia nigra presented with the highest histological scores for the monkeys inoculated i.c. for all viruses. Based on the individual values shown in Table 3, monkeys inoculated with the 17DD virus had average scores in this area of 1.75 (experiment I) and 1.95 (experiment II), compared to 1.40 for 17D/13 and 1.80 for 17D/8, respectively. Monkey T45 presented grade-3 lesions in the target area and succumbed to infection. In five MNVTs for the 17DD 102/84 seed lot virus, from which our control 17DD virus was produced, all animals showing that much neuronal involvement in the target area had died before the experimental period was over. The average target area score in these tests was 1.49 (15).

Among the discriminator areas in the CNS, the putamen, globus pallidus, and nucleus caudatus were the areas most affected, but the lesion scores were never above 2 with any of the viruses in experiment I. However, in experiment II, several animals showed grade-3 lesions in at least one (but not simultaneously in all) hemisection of the above areas and the nuclei thalami. These included monkeys T21, T25, T45, T57, T81, and U11, inoculated with the YF 17DD virus, as well as monkey T63, inoculated with 17D/8. Monkey T45 presented grade-3 lesions in the target area, the globus pallidus, and the lumbar enlargement of the spinal cord. Monkey 6U, inoculated with 17D/13, presented the highest clinical score (1.00) among the 20 animals in experiment I and showed the third-lowest score in the discriminatory areas (0.33 [Table 3]). The average discriminator area score for the 17DD virus was 0.78, compared with 0.53 for 17D/13. In experiment II, monkey T45 had the highest discriminator area score (1.62), well above the mean of 1.02 for the 17DD group. Monkey T63, inoculated with 17D/8, had the highest scores for both target and discriminator areas for the group inoculated with this virus, yet no clinical signs were noted.

TABLE 4. Nucleotide sequence comparison of YF 17D viruses

| Position[a] | Nucleotide in the following virus: | | | Amino acid effect |
|---|---|---|---|---|
| | 17D/8[b] | 17D/13[b] | 17D-204 | |
| 1703 (E244) | T | G | G | T = L; G = V |
| 1946 (E325) | T | C | T | T = S; C = P |
| 2219/20 (E416) | A/C | G/T | A/C | A/C = T; G/T = V |
| 2356 | T | C | T | |
| 2449 | C | C | G | |
| 2452 | C | C | G | |
| 2602 | T | C | T | |
| 2677 | C | T | C | |
| 2681 (NS1 87) | G | A | G | G = A; A = T |
| 4025 (NS2A 173) | A | A | G | A = M; G = V |
| 5641 | G | G | A | |
| 6529 | C | C | T | |
| 6758 (NS4A 107) | G | G | A | G = V; A = I |
| 8212 | T | T | C | |
| 8656 | C | C | A | |
| 8808 (NS5 391) | G | G | A | G = S; A = N |
| 9605 (NS5 657) | A | A | G | A = N; G = D |
| 10722 | G | G | A | |

[a] Numbering according to GenBank accession number X03700.
[b] Viral stocks at third passage level.

Assessment of the histological basis of the neurotropism of a given virus is based on the average of the combined target and discriminator area scores of all monkeys. For the 17DD virus, this combined score was 1.21, whereas for 17D/13 it was 0.96. Given the normal distribution presented by the individual values in this test, we used the *t* test to analyze the significance of the difference between the two means. The mean for the 17D/13 virus is at the borderline level of significance ($P = 0.05$), suggesting a more attenuated phenotype for this virus than for 17DD. In experiment II, the combined scores for the monkeys inoculated with 17D/8 are lower than those for the group that received the control 17DD virus (1.23 versus 1.48 [Table 3]), suggesting a higher degree of attenuation for the former. Both parametric (*t*) and nonparametric (Kruskal-Wallis) tests indicated a statistically significant difference between the means ($P = 0.03$).

**Recombinant virus genetic stability.** As previously reported, the insertion $GG(NANP)_3GG$ of the YF 17D/8 virus was stable after serial passages in Vero cells but not in chicken embryo fibroblasts (1). We performed two independent serial passages of the YF 17D/13 virus at passage 3 in Vero cells, with an MOI of 0.02. After sequencing the respective genomic area at the fifth and tenth passages, we observed that the insertion (SYVPSAEQI) was intact.

A total of 19 positions were found to differ between the YF 17D-204 virus and the 17D/8 and 17D/13 viruses, leading to eight amino acid substitutions (Table 4). The YF 17D/8 virus and 17D/13 differed at eight nucleotide positions and four amino acid residues, three of which were in the E protein at amino acids E244, E325, and E416. The remaining substitution was in the NS1 gene (NS1 87). With the exception of the

change at E244, which is due to mutation during the viral passages, all reflect the use of a different plasmid DNA background for virus regeneration. Mutations at positions 4025 (NS2A 173), 6758 (NS4A 107), 8808 (NS5 391), and 9605 (NS5 657) are common to the two recombinant viruses and differ from 17D-204. The former two mutations reflect clonal differences between the cDNA used for the sequencing (24), GenBank accession number X00730, and that used for the cloning and virus regeneration described here. The two changes at NS5 were introduced by mutagenesis of the original infectious cDNA (23) and were present in the plasmids used to regenerate both the 17D/8 and 17D/13 viruses but were absent from the original sequence.

## DISCUSSION

The YF 17D virus has several characteristics which are desirable for new live attenuated vaccines. We have approached its development as a vector for heterologous antigens by studying the expression of a humoral epitope at the surface of the E protein based on the results of modeling of its three-dimensional structure. A recombinant virus expressing a B-cell epitope from the malarial parasite *Plasmodium falciparum* was characterized with regard to surface expression of the epitope, viral growth, attenuation for mice, and immunogenicity (1). Here we describe the construction and characterization of a second 17D recombinant virus expressing a $CD8^+$ T-cell determinant. This epitope is present in the major circumsporozoite surface protein of *Plasmodium yoelii* and has been shown to confer protection on mice challenged with live sporozoites (28). The insertions were made in the *fg* loop, located in domain II of the 3D structure proposed for the E protein, a domain not known to be involved in cell tropism and possibly virulence. Here we demonstrate experimentally that insertions at this site do not compromise viral attenuation.

One of the hallmarks of the YF 17D vaccine is its extremely low incidence of adverse events. A total of 21 cases of neurological disease have been reported (19), and encephalitic reactions in vaccinees were also observed in the early development of the YF 17D virus (4). Since neurotropism is a concern with YF 17D vaccines, a standardized neurovirulence test with monkeys was established to ensure the attenuation of any YF 17D virus (12, 30). The attenuation of the recombinant 17D/8 and 17D/13 viruses was rigorously studied in tests for neurotropism and viscerotropism in rhesus monkeys, as recommended for YF 17D vaccine viruses (30). Since the YF 17DD virus has a long history of safe use in humans, we used it as a reference against which to compare the recombinant viruses in the MNVT.

Vaccine-related clinical signs were observed in 12 out of 20 monkeys that received the YF 17DD virus beginning at day 8 postinoculation and included encephalitis in some animals. In contrast, clinical signs were observed for only 1 monkey out of 10 that received the 17D/8 virus and were minor. Virus-related clinical signs were observed for only 2 out of 10 animals that received the 17D/13 virus. Accordingly, the clinical score for the group of monkeys that received the 17D/8 virus was significantly lower than that for the group inoculated with the 17DD vaccine. The group that received the 17D/13 virus did not show a significantly different clinical score from the group receiving 17DD. Likewise, the histological lesions in both target and discriminatory areas of monkeys inoculated with the recombinant 17D viruses were less frequent and of lower intensity, involving fewer neuronal changes and yielding combined histological scores significantly lower than those observed for the control YF 17DD vaccine virus. Although the YF 17DD virus was recently found to be slightly more neurovirulent for rhesus monkeys than 17D-204, the histological scores for the recombinant viruses were similar to those observed for YF-VAX, a commercial 17D-204-based vaccine (20).

Viscerotropism was assessed by measuring viremia after i.c. inoculation and analyzing slides of the liver, spleen, heart, kidney, and adrenal glands from all monkeys by light microscopy. The amount of 17D virus in the extraneural circulation must be below 500 mouse $LD_{50}$/0.03 ml for all (10 out of 10) sera and $\geq$100 $LD_{50}$/0.03 ml in 1 out of 10 monkey sera at a 1:10 dilution. In this regard, the highest viremia observed was 2.42 $\log_{10}$ PFU/ml for monkey 810, inoculated with 17DD. That corresponds to 1.64 $LD_{50}$/0.03 ml, well below the established limits. In addition, the range of titers observed here is similar to that observed for rhesus monkeys inoculated with the attenuated 17D/JE SA-14-14-2 virus or with the chimeric 17D-den or 17D-204 virus (7, 8, 20). In addition, no evidence for hepatic, renal, or myocardial dysfunction or pathology was found, suggesting the absence of any unexpected tissue tropism or altered pathogenesis.

The observations of limited viremia, minimal clinical signs of infection, no extraneural organ alterations, and CNS histological scores within the expected range all suggest an attenuated phenotype for the YF 17D/8 and 17D/13 recombinant viruses. If the *fg* loop is to be employed in a predictable fashion for the production of recombinant viruses carrying other heterologous epitopes, the destabilization of the E protein 3D structure, interference with the threshold for the dimer-to-trimer transition, and alteration of the fusion activation itself should be considered as potentially involved in viral overattenuation and reduced immunogenicity.

The *fg* loop is located in domain II of the 3D structure of the E protein of flaviviruses (22). This domain is highly cross-linked by disulfide bonds and undergoes a low-pH transition, which is related to exposing a strictly conserved and hydrophobic stretch of amino acids involved in the fusion of the viral envelope to the endosomal membrane. This transition involves a rearrangement of the E protein dimers into trimers, together with a simultaneous conformational change within each monomer, which leads to a novel spatial distribution of the three domains (2, 18). In order for this to occur, the molecule possesses inherent flexibility at the interface between domains I and II, particularly due to the *kl* loop. In the models for the 17D/13 virus, the conformation of this loop appears to be perturbed by that of the insert itself, which lies spatially close by. The overall increase in the hidden surface area (217 $Å^2$) and the potential for a greater number of hydrogen bonds across the dimer interface as a result of the insert may inhibit the transition from dimer to trimer necessary for infection. Alterations to specific interactions at the dimer interface have been put forward recently by Guirakhoo et al. (8) as an explanation for the attenuation conferred by a single point mutation within the *fg* loop of a chimeric YF 17D-dengue 1 virus. However, in the case of 17D/8, the hypothesis of an altered transi-

tion threshold is less appealing, because the insert, despite its size, is predicted to interfere only minimally with the dimer interface and the *kl* loop, due to the presence of the glycine spacers, which lift the $(NANP)_3$ epitope above the surface of the virus (1). The most likely explanation would, therefore, appear to be related to the fusion activity itself.

Upon superposition of domain II of the models onto the same region of one of the monomers within the postfusion trimer (2) the *fg* loop continues to be solvent exposed and therefore is not expected to interfere with trimer formation. However, it has been postulated that, for fusion to occur, a ring of such trimers must form so that the fusion peptides at their tip are brought into close proximity (2, 18), in a manner similar to that observed for alphaviruses such as Semliki Forest virus (6). This requires that the lateral surfaces of the trimers must approach one another. As can be seen from Fig. 3, a large insert in the *fg* loop (such as is present in 17D/8) would sterically impede this approach, compromising the capability of the E protein to induce fusion of viral and endosomal membranes. It is conceivable that a lower rate of fusion may delay the extent of virus production and thereby lead to a milder infection of the host, accounting for the lower extent of replication in cultured cells and the more attenuated phenotype of the recombinant virus in both the mouse and monkey models. Although the protrusion of the 17D/13 loop is less marked and presumably more readily tolerated, it may contribute to attenuation in this case also.

It is of interest that the 17D/13 and 17D/8 viruses differ at specific amino acid positions in the genome. Three of these positions are located in the E protein, two (at positions 244 and 325) within the soluble domain. 17D/13 bears a proline at position 325 compared with a serine in 17D/8. This is not expected to contribute significantly to their different phenotypes, as this difference is also observed between the 17D-204 and 17DD vaccine strains. However, the possibility cannot be totally ruled out, as this position maps to the predicted receptor binding site on domain III. From the 3D structure, the difference at position 244 (leucine in 17D/8 and valine in 17D/13) seems unlikely to contribute to the phenotypic differences observed here, due to both its conservative nature and the additional space afforded to the hydrophobic cavity at this amino acid position by the presence of an alanine at 117 (compared with valine in TBE), which would aid in accommodating either the larger leucine at 244 or the valine more commonly seen in flavivirus sequences. There are five other amino acid changes (Table 4), the role of which in viral attenuation remains unclear. It is noteworthy that the substitution at NS5 657 is close to the GDD motif of viral RNA polymerases and may have some effect on viral RNA replication.

The fact that all monkeys mounted a neutralizing antibody response against the YF 17D/13 virus and that 9 out of 10 mounted such a response against 17D/8 suggests that the recombinant viruses have maintained their immunogenicity, despite the epitope insertions in the envelope protein. However, the mean neutralizing antibody titers for both recombinant viruses were significantly lower than those elicited by the 17DD vaccine virus. The fact that both viruses are neutralized efficiently by YF-immune monkey and mouse sera suggests that the projection of the longer *fg* loop from the external surface of the dimer would cause minimal steric hindrance to antibody binding at the external surface of the E protein domain II, where important flavivirus B-cell epitopes are located (9, 14). The most plausible explanation for the reduced immunogenicity is the limited viral replication. We are currently examining the capability of the 17D/8 virus to elicit a humoral immune response after subcutaneous inoculation of rhesus monkeys.

The results shown here suggest that inserts of different sizes and amino acid compositions are tolerated at the YF 17D virus E protein *fg* loop. This is consistent with the 3D structures of both the dimeric and trimeric forms, in which the *fg* loop lies exposed to solvents (Fig. 3 and 4). The insert design was originally based on the crystal structure of the dimer, and the site was chosen so as to minimally interfere with its lateral surface, as this would be expected to perturb the assembly of the 90 dimers into the complete envelope. The recent determination of the postfusion, low-pH form of the E protein from TBE and dengue viruses indicates that the external surface of domain II in the dimer, where *fg* resides, has become the lateral surface in the trimer (Fig. 4). As described above, this may impose steric restraints on trimer approximation during envelope fusion. Although the *fg* loop may therefore represent a tolerant generic insertion site in structural terms, there may be limitations to its use which may restrict the size of the peptide that can be accommodated without causing a significant loss in functionality.

The testing of both recombinant viruses (17D/8 and 13) for monkey neurovirulence also suggests that insertion at the 17D E protein *fg* loop does not compromise the attenuated phenotype of the YF 17D virus further, confirming the potential use of this site for the insertion of foreign epitopes and the development of new live attenuated 17D virus-based vaccines.

Malaria remains one of the most important vector-borne human diseases. The concept that vaccination may be a useful tool to control the disease is based mainly on the fact that individuals continually exposed to infection by the parasitic protozoan eventually develop immunity to the disease. It is noteworthy that immunization of humans with a single dose of YF 17D virus suffices to induce detectable levels of neutralizing antibodies to YF virus even 40 years after the primary immunization (19), a fact that lends further support to the use of the 17D virus to express the relevant malarial epitopes toward the development of a new line of viral vaccines capable of protecting against both diseases, possibly on a lifelong basis. In this regard the immunization of mice with the 17D/13 virus carrying the CD8 epitope induced significant T-cell priming, which contributed to a high degree of protection against a sporozoite challenge (R. S. Nussenzweig; M. C. Bonaldo, and R. Galler, unpublished results). The attenuation of YF 17D/8 virus shown here warrants the use of this virus in the formulation of a multicomponent vaccine, including viruses expressing T-cell epitopes from human plasmodia toward the induction of antiparasite immunity.

While it is true that single epitopes might not counter an infection by a malaria parasite, which is made up of different proteins during the various stages of its life cycle, over the last decades different groups have described several epitopes related to all arms of the immune response. There have also been efforts to develop strings of epitopes as new candidate vaccines. For YF 17D virus, the *fg* loop will probably accommodate only single epitopes, with structural restrictions on size

and amino acid composition, but the expression of a protective parasite epitope between NS2B and NS3 has recently been accomplished (27). Therefore, one can envisage that multiple epitopes can be inserted into different areas of the genome depending on their immunological specificity. Humoral epitopes could be expressed at the *fg* loop of the virion surface and T-cell epitopes between NS2B and NS3, given their cytoplasmic location, facilitating their presentation in the class I or II context. In addition, vaccines against these parasites will most certainly rely on the formulation of different 17D viruses expressing different epitopes in order to induce sterile immunity or protection against the parasite.

On the other hand, an important parasite life stage, the merozoite, which infects red blood cells, has had a number of antigens well characterized. However, none of these are small epitopes. A successful malaria vaccine will probably rely on immunity to both stages of the life cycle: the sporozoite, the source of the CS protein epitopes we have described here, and the merozoite. Therefore, new strategies for expressing larger protein domains by YF 17D virus are being sought.

## ACKNOWLEDGMENTS

We thank the Instituto de Tecnologia em Imunobiológicos (Bio-Manguinhos) for continuing interest in this work and Edney do Monte, Idevaldo I. Ferreira, José M. da Silva, and André L. B. Ambrósio for technical support. We also thank Joel Majerowicz for the use of animal facilities.

Financial support from ICGEB, WHO/TDR, CNPq, FAPERJ, FAPESP, PDTIS/FIOCRUZ, and PAPES/FIOCRUZ is gratefully acknowledged.

## REFERENCES

1. **Bonaldo, M. C., R. C. Garratt, P. S. Caufour, M. S. Freire, M. M. Rodrigues, R. S. Nussenzweig, and R. Galler.** 2002. Surface expression of an immunodominant malaria protein B cell epitope by yellow fever virus. J. Mol. Biol. **315:**873–885.
2. **Bressanelli, S., K. Stiasny, S. L. Allison, E. A. Stura, S. Duquerroy, J. Lescar, F. X. Heinz, and F. A. Rey.** 2004. Structure of a flavivirus envelope glycoprotein in its low-pH-induced membrane fusion conformation. EMBO J. **23:** 728–738.
3. **Caufour, P. S., M. C. Motta, A. M. Yamamura, S. Vazquez, I. I. Ferreira, A. V. Jabor, M. C. Bonaldo, M. S. Freire, and R. Galler.** 2001. Construction, characterization and immunogenicity of recombinant yellow fever 17D-dengue type 2 viruses. Virus Res. **79:**1–14.
4. **Fox, J. P., E. H. Lennette, C. Manso, and J. R. Souza Aguiar.** 1942. Encephalitis in man following vaccination with 17D yellow fever virus. Am. J. Hyg. **36:**117–142.
5. **Galler, R., K. V. Pugachev, C. L. Santos, S. W. Ocran, A. V. Jabor, S. G. Rodrigues, R. S. Marchevsky, M. S. Freire, L. F. Almeida, A. C. Cruz, A. M. Yamamura, I. M. Rocco, E. S. da Rosa, L. T. Souza, P. F. Vasconcelos, F. Guirakhoo, and T. P. Monath.** 2001. Phenotypic and molecular analyses of yellow fever 17DD vaccine viruses associated with serious adverse events in Brazil. Virology **290:**309–319.
6. **Gibbons, D. L., I. Erk, B. Reilly, J. Navaza, M. Kielian, F. A. Rey, and J. Lepault.** 2003. Visualization of the target-membrane-inserted fusion protein of Semliki Forest virus by combined electron microscopy and crystallography. Cell **114:**573–583.
7. **Guirakhoo, F., K. Pugachev, Z. Zhang, G. Myers, I. Levenbook, K. Draper, J. Lang, S. Ocran, F. Mitchell, M. Parsons, N. Brown, S. Brandler, C. Fournier, B. Barrere, F. Rizvi, A. Travassos, R. Nichols, D. Trent, and T. Monath.** 2004. Safety and efficacy of chimeric yellow fever-dengue virus tetravalent vaccine formulations in nonhuman primates. J. Virol. **78:**4761–4775.
8. **Guirakhoo, F., Z. Zhang, G. Myers, B. W. Johnson, K. Pugachev, R. Nichols, N. Brown, I. Levenbook, K. Draper, S. Cyrek, J. Lang, C. Fournier, B. Barrere, S. Delagrave, and T. P. Monath.** 2004. A single amino acid substitution in the envelope protein of chimeric yellow fever-dengue 1 vaccine virus reduces neurovirulence for suckling mice and viremia/viscerotropism for monkeys. J. Virol. **78:**9998–10008.
9. **Holzmann, H., K. Stiasny, H. York, F. Dorner, C. Kunz, and F. X. Heinz.** 1995. Tick-borne encephalitis virus envelope protein E-specific monoclonal antibodies for the study of low pH-induced conformational changes and immature virions. Arch. Virol. **140:**213–221.
10. **Lai, C. J., and T. P. Monath.** 2003. Chimeric flaviviruses: novel vaccines against dengue fever, tick-borne encephalitis, and Japanese encephalitis. Adv. Virus Res. **61:**469–509.
11. **Laskowski, R. A., M. W. MacArthur, D. S. Moss, and J. M. Thornton.** 1993. Procheck—a program to check the stereochemical quality of protein structures. J. Appl. Crystallogr. **26:**283–291.
12. **Levenbook, I. S., L. J. Pelleu, and B. L. Elisberg.** 1987. The monkey safety test for neurovirulence of yellow fever vaccines: the utility of quantitative clinical evaluation and histological examination. J. Biol. Stand. **15:**305–313.
13. **Luthy, R., J. U. Bowie, and D. Eisenberg.** 1992. Assessment of protein models with three-dimensional profiles. Nature **356:**83–85.
14. **Mandl, C. W., F. Guirakhoo, H. Holzmann, F. X. Heinz, and C. Kunz.** 1989. Antigenic structure of the flavivirus envelope protein E at the molecular level, using tick-borne encephalitis virus as a model. J. Virol. **63:**564–571.
15. **Marchevsky, R. S., M. S. Freire, E. S. Coutinho, and R. Galler.** 2003. Neurovirulence of yellow fever 17DD vaccine virus to rhesus monkeys. Virology **316:**55–63.
16. **Marchevsky, R. S., J. Mariano, V. S. Ferreira, E. Almeida, M. J. Cerqueira, R. Carvalho, J. W. Pissurno, A. P. da Rosa, M. C. Simoes, and C. N. Santos.** 1995. Phenotypic analysis of yellow fever virus derived from complementary DNA. Am. J. Trop. Med. Hyg. **52:**75–80.
17. **Modis, Y., S. Ogata, D. Clements, and S. C. Harrison.** 2003. A ligand-binding pocket in the dengue virus envelope glycoprotein. Proc. Natl. Acad. Sci. USA **100:**6986–6991.
18. **Modis, Y., S. Ogata, D. Clements, and S. C. Harrison.** 2004. Structure of the dengue virus envelope protein after membrane fusion. Nature **427:**313–319.
19. **Monath, T.** 2003. Yellow fever vaccine, 4th ed. W. B. Saunders Company, Philadelphia, Pa.
20. **Monath, T. P., I. Levenbook, K. Soike, Z. X. Zhang, M. Ratterree, K. Draper, A. D. Barrett, R. Nichols, R. Weltzin, J. Arroyo, and F. Guirakhoo.** 2000. Chimeric yellow fever virus 17D-Japanese encephalitis virus vaccine: dose-response effectiveness and extended safety testing in rhesus monkeys. J. Virol. **74:**1742–1751.
21. **Rey, F. A.** 2003. Dengue virus envelope glycoprotein structure: new insight into its interactions during viral entry. Proc. Natl. Acad. Sci. USA **100:** 6899–6901.
22. **Rey, F. A., F. X. Heinz, C. Mandl, C. Kunz, and S. C. Harrison.** 1995. The envelope glycoprotein from tick-borne encephalitis virus at 2 Å resolution. Nature **375:**291–298.
23. **Rice, C. M., A. Grakoui, R. Galler, and T. J. Chambers.** 1989. Transcription of infectious yellow fever RNA from full-length cDNA templates produced by in vitro ligation. New Biol. **1:**285–296.
24. **Rice, C. M., E. M. Lenches, S. R. Eddy, S. J. Shin, R. L. Sheets, and J. H. Strauss.** 1985. Nucleotide sequence of yellow fever virus: implications for flavivirus gene expression and evolution. Science **229:**726–733.
25. **Sali, A., and T. L. Blundell.** 1993. Comparative protein modelling by satisfaction of spatial restraints. J. Mol. Biol. **234:**779–815.
26. **Stefano, I., H. K. Sato, C. S. Pannuti, T. M. Omoto, G. Mann, M. S. Freire, A. M. Yamamura, P. F. Vasconcelos, G. W. Oselka, L. W. Weckx, M. F. Salgado, L. F. Noale, and V. A. Souza.** 1999. Recent immunization against measles does not interfere with the sero-response to yellow fever vaccine. Vaccine **17:**1042–1046.
27. **Tao, D., G. Barba-Spaeth, U. Rai, V. Nussenzweig, C. M. Rice, and R. S. Nussenzweig.** 2005. Yellow fever 17D as a vaccine vector for microbial CTL epitopes: protection in a rodent malaria model. J. Exp. Med. **201:**201–209.
28. **Tsuji, M., C. C. Bergmann, Y. Takita-Sonoda, K. Murata, E. G. Rodrigues, R. S. Nussenzweig, and F. Zavala.** 1998. Recombinant Sindbis viruses expressing a cytotoxic T-lymphocyte epitope of a malaria parasite or of influenza virus elicit protection against the corresponding pathogen in mice. J. Virol. **72:**6907–6910.
29. **Vriend, G.** 1990. WHAT IF: a molecular modeling and drug design program. J. Mol. Graph. **8:**52–56, 29.
30. **World Health Organization.** 1998. Requirements for yellow fever vaccine. WHO Tech. Rep. Ser. **872:**31–68.